Current Research in Microbial Sciences 8 (2025) 100364

Contents lists available at ScienceDirect

Current Research in Microbial Sciences

journal homepage: www.sciencedirect.com/journal/current-research-in-microbial-sciences

Heptad repeat 1-derived N peptide inhibitors improve broad-spectrum anti-HIV-1 activity

Chen Yuan [a,1], Jia-Ye Wang [a,b,1], Bu-Yi Wang [a], Yi-Lin Zhao [a], Yan Li [a,b,c], Di Li [a,b,c], Hong Ling [a,b,c,*], Min Zhuang [a,b,c,*]

[a] Department of Microbiology, Harbin Medical University, Harbin, 150081, China
[b] Heilongjiang Provincial Key Laboratory of Infection and Immunity, Harbin, 150081, China
[c] Key Laboratory of Pathogen Biology, Harbin, 150081, China

ARTICLE INFO

Keywords:
HIV-1
HR1
HR2
N peptide inhibitor
N36
IZN36
FPPR
MTQ

ABSTRACT

Background: HIV-1 N-peptide inhibitor (NPI) derived from N-terminal heptad-repeat region (HR1) of gp41 can target C-terminal heptad-repeat region (HR2) or the HR1 to interfere with the formation of endogenous six-helix bundle (6HB). However, the NPI is less active than the C-peptide inhibitor. In this study, we reported three HR1-derived NPIs designed by adding fusion peptide proximal region (FPPR) of gp41 or a trimeric motif MTQ into the N36 peptide and then evaluated their anti-HIV-1 activities.

Methods: Molecular modeling was performed using Swiss Model. The inhibitory activity of NPIs on HIV-1 was assessed by Env-pseudovirus infection assays and cell-cell fusion assays. Interaction between NPIs and HR2 peptides was evaluated by circular dichroism and Native PAGE.

Results: The three newly designed NPIs, FPPR-N36, MTQ-N36, and MTQ-FPPR-N36, exhibited higher anti-HIV-1 activity than N36. The stability of the coiled-coil core formed by three designed NPIs or the 6HB formed by C34 and these NPIs were significantly higher than those of corresponding monomer N36 or isoleucine zipper-engineered trimeric N36 (IZN36). The 50 % inhibitory concentrations (IC_{50}) of MTQ-N36 against HIV-1 infection were at a nanomolar level, lower than those of other tested NPIs. The FPPR-N36 could also inhibit infection of HIV-1 strains that were resistant to N36 and IZN36.

Conclusions: The three newly designed NPIs had inhibitory activity against HIV-1 infection. Among them, MTQ-N36 exhibited a higher potential to inhibit HIV-1 entry than other peptides, and FPPR-N36 might be a promising candidate NPI for suppressing HIV-1 strains that are resistant to conventional NPIs.

Abbreviations

Env	Envelope protein
gp41	HIV envelope transmembrane subunit
gp120	HIV envelope surface subunit
HR1	N-terminal heptad repeat
HR2	C-terminal heptad repeat
FPPR	fusion peptide proximal region
6HB	six-helix bundle
CD	circular dichroism
Native PAGE	native polyacrylamide gel electrophoresis
Tm	transition mid-point temperature

1. Introduction

The envelope glycoprotein (Env) of human immunodeficiency virus type 1 (HIV-1) consists of surface subunit gp120 and transmembrane subunit gp41, with noncovalent association in the viral membrane (Wyatt et al., 1998). The HIV-1 entry process offers numerous possibilities for preventing viral infection. Gp120 binds to CD4 molecules in target cells and then interacts with a chemokine receptor, CCR5 or CXCR4, to further bring the virus membrane and the cell membrane closer together (Pancera et al., 2010, Huang et al., 2005, Zhou et al., 2007). The triggered conformational changes allow the fusion peptide, which is composed of approximately 20 residues at the hydrophobic N-terminal region of gp41, to insert into the membrane of target cells,

* Corresponding authors.
E-mail addresses: lingh@ems.hrbmu.edu.cn (H. Ling), zhuangm@ems.hrbmu.edu.cn (M. Zhuang).
[1] These authors contributed equally to this work.

https://doi.org/10.1016/j.crmicr.2025.100364

Available online 21 February 2025

forming a transiently pre-hairpin intermediate (Kwong et al., 1998, Pancera et al., 2014, Buzon et al., 2010). Subsequently, the gp41 N-terminal heptad-repeat (HR1) forms a coiled-coil core, and the C-terminal heptad-repeat (HR2) refolds and interacts with HR1 in an antiparallel manner to form a thermostable six-helix bundle (6HB) (Chan et al., 1997, Lu and Kim, 1997, Caffrey, 2001, Markosyan et al., 2003). This process draws target cells and viral membranes closely and facilitates fusion pore formation to allow viral genes to penetrate into cells (Eckert and Kim, 2001). The fusion peptide inhibitors targeting HR1 or HR2 can interrupt this process, thereby blocking virus entry (Nelson et al., 2007, Caffrey, 2011).

Fusion peptide inhibitors against HIV-1 are synthetic peptides that are derived from the gp41 HR1 or HR2 (Wild et al., 1993, Jiang et al., 1993, Moore and Doms, 2003, He, 2013). HR2-derived C-peptide inhibitor (CPI) binds to the pre-hairpin intermediate of HR1 and forms a heterogenous 6HB to hinder the formation of endogenous 6HB. T20 (enfuviride or Fuzeon) was the first approved CPI that was applied to the clinic (Baldwin et al., 2004, Joly et al., 2010, McGillick et al., 2010). However, the rapid appearance of HIV-1 resistant mutations and the short half-life of T20 limited its widespread applications. Further, the modified CPIs with increased binding ability, bioavailability, and inhibition effect were developed (AIDS et al., 2004, Dwyer et al., 2007, Nishikawa et al., 2008, Chong et al., 2012, Chong et al., 2012, Chong et al., 2014, Zheng et al., 2014, Chong et al., 2015, Chong et al., 2015, Chong et al., 2016, Chong et al., 2017, Ding et al., 2017, Xue et al., 2022), and one of them, Albuvirtide, was approved for clinical use in China (Chong et al., 2012). The common escape mutations from CPIs were found in the specific residues of HR1, resulting in low or no binding of CPIs to the HR1 trimer. Besides, additional mutations in gp41 HR2 can adapt to the change of HR1 residues to increase viral endogenous 6HB formation (Greenberg and Cammack, 2004, Wild et al., 1994, De Feo and Weiss, 2012, Liu et al., 2011, Lu et al., 2006).

HR1 sequences from HIV isolates worldwide are highly conservative across HIV subtypes and were used for designing monomeric and trimeric N peptide inhibitors (NPIs). However, the poor solubility and low bioavailability (with the 50 % inhibitory concentration, IC_{50}, at the micromolar level) of N36 (corresponding to residues 546–581 in HXB2 Env) are still the major problems to be solved (Eckert and Kim, 2001, Izumi et al., 2010). IZN36, which is composed of the monomeric N36 and a trimer motif, isoleucine zipper (IZ), exhibited a significant improvement in solubility and inhibitory potency (with the IC_{50} at nanomolar level), than N36 (Eckert and Kim, 2001, Izumi et al., 2010). The pathways of HIV resistance to N36 revealed that HR1-derived NPIs target two sites of gp41 (Zhuang et al., 2019, Zhuang et al., 2012, Shu et al., 2000, He et al., 2008). It can interact with gp41 HR1 to form a heterotrimeric coiled-coil core, or can also spontaneously form an NPI trimer to bind to HR2, thereby interfering with the formation of an endogenous 6HB (Bewley et al., 2002). Although the NPIs, such as N36 Mut(e, g), N35CCG-N13, and covNHR3 (Bewley et al., 2002, Louis et al., 2003, Crespillo et al., 2014), modified by amino acid mutation(s), chemical bonds, or linker, increased inhibition potency than N36, the inhibitory effects of these peptides on the resistance stains to N36 and trimeric N36 inhibitors were not evaluated. Therefore, the optimization of NPIs to improve their solubility and bioavailability, thereby increasing their inhibitory effects on HIV-1 infection is the current main research direction in this field.

In the previous study, we found that HIV-1 X 4 and R5 tropic viruses can use a similar resistance mechanism (improving the thermostability of 6HB) to escape from NPIs, but use different gp120-gp41 interactions to regulate Env conformational changes (Zhuang et al., 2019, Zhuang et al., 2012). Both resistant viruses selected two genetic pathways that contain an early mutation in HR1 or HR2 with equal probability to escape from N36 and preferentially selected the HR1 pathway to escape from IZN36. We found that among these mutations, E560 in HR1 is a mutation hotspot to escape NPIs and CPIs (Yuan et al., 2019). Interestingly, under N36 selection, some NPIs-resistant viruses are difficult to culture to increase the resistant degree, implying that the resistant mutations to NPI monomer confer limited resistance levels. Meanwhile, we found that the thermostability of 6HB is the key mechanism to escape from NPIs.

In the present study, to increase the NPI solubility and thermostability of 6HB, N36, a commonly-used NPI, was modified by introducing the fusion peptide proximal region (FPPR) and/or a trimer motif MTQ which was designed by our group previously (Wang et al., 2011), aiming to increase the inhibitory potency of NPIs. The three newly designed NPIs (FPPR-N36, MTQ-N36 and MTQ-FPPR-N36) showed more potent inhibitory effects against HIV-1 entry than N36. The MTQ-N36 trimer showed slightly better inhibitory activity against HIV-1 entry than the isoleucine zipper-engineered N36 trimer (IZN36). FPPR-N36 can inhibit wild-type HIV strains as well as the strains resistant to N36 or IZN36 as well as wild-type HIV. Our findings provided new insights for designing more broad-spectrum and effective NPIs.

2. Materials and methods

2.1. Cells and plasmids

HEK293T cell was purchased from America ATCC. TZM-bl cell was obtained from NIH AIDS Reagent Program. RC4 cell that expresses low levels of CD4 and CCR5 was a gift from David Kabat (Oregon Health and Science University, Portland, OR) (Platt et al., 1998). The expression vector pCMV/R and the Env-deficient HIV-1 backbone plasmid pSG3Δenv were provided by Gary Nabel (National Institutes of Health, Bethesda, MD). The plasmids pSCTZ-α, pSCTZ-ω and pRev were provided by Dan Littman (New York University), the plasmids pcDNA3.1-BJ-28–13, pcDNA3.1-BJX-4.6 and pSV7d-SH188.6 were provided by YC Wang (the China Academy of Food and Drug Administration), and the plasmids pCMV/R-LAI, pCMV/R-JRcsf, pCMV/R-09, 277-R9, pCMV/R-06,057-C3, pcDNA3.1–06,044–7, pCMV/R-JRcsf E560K/Q577R/T641I and pCMV/R-JRcsf Q577R/E648 K were constructed by our group.

2.2. Synthetic peptides

All the amino acid residues were numbered according to the HXB2 Env protein. N36 (residues 546–581; SGIVQQQNNLLRAIEAQQHLLQLTVWGIKQLQARIL), FPPR-N36 (residues 536–581; TLTVQARQLLSGIVQQQNNLLRAIEAQQHLLQLTVWGIKQLQARIL), MTQ-N36 (KIKEEQAKIKEKIAEIEKRISGIVQQQNNLLRAIEAQQHLLQLTVWGIKQLQARIL), MTQ-FPPR-N36 (KIKEEQAKIKEKIAEIEKRIVQARQLLSGIVQQQNNLL

Table 1
Peptide inhibitor sequences.

Peptide inhibitors	Peptide sequence
N36	SGIVQQQNNLLRAIEAQQHLLQLTVWGIKQLQARIL
FPPR-N36	TLTVQARQLLSGIVQQQNNLLRAIEAQQHLLQLTVWGIKQLQARIL
IZN36	IKKEIEAIKKEQEAIKKKIEAIEKEISGIVQQQNNLLRAIEAQQHLLQLTVWGIKQLQARIL
MTQ-N36	KIKEEQAKIKEKIAEIEKRISGIVQQQNNLLRAIEAQQHLLQLTVWGIKQLQARIL
MTQ-FPPR-N36	KIKEEQAKIKEKIAEIEKRIVQARQLLSGIVQQQNNLLRAIEAQQHLLQLTVWGIKQLQARIL
C34	WMEWDREINNYTSLIHSLIEESQNQQEKNEQELL

RAIEAQQHLLQLTVWGIKQLQARIL), IZN36 (IKKEIEAIKKEQEAIKKKIEAIEKEISGIVQQQNNLLRAIEAQQHLLQLTVWGIKQLQARIL) (Eckert and Kim, 2001) and C34 (residues 628–661; WMEWDREINNYTSLIHSLIEESQNQQEKNEQELL) were synthesized by Shanghai JiEr Biochemistry Company (Table 1).

2.3. Peptide design and structure prediction

We designed three new NPIs based on N36 peptide. The spatial conformation of NPIs was predicted by SWISS Model (https://swissmodel.expasy.org/), and the molecular conformation of NPIs was analyzed by PyMOL software (Schrödinger, NY).

2.4. Cytotoxicity analysis of NPIs

The cytotoxicity of peptides was determined in TZM-bl cell using a Cell Counting Kit-8 (CCK-8) assay (Meilunbio, Dalian, China). In brief, a total of 1×10^4 TZM-bl cells were seeded on a 96-well tissue culture plate, and then the FPPR-N36, MTQ-N36, or MTQ-FPPR-N36 peptides diluted at graded concentrations were added to the cells. After incubation of the plate at 37 °C for 48 h, 10 μL of CCK-8 solution reagent was added into each well and the plate was incubated for 2 h at 37 °C. The absorbance at 450 nm (OD_{450}) was measured using the Model 550 Microplate Reader (Bio-Rad, CA).

2.5. HIV-1 Env-pseudovirus inhibition assay

The HIV-1 Env pseudoviruses were generated by the co-transfection with 0.075 μg (pCMV/R vector) or 1 μg (pcDNA3.1 or pSV-7d vector) of the Env-expressing plasmid, 2 μg of Env-deficient HIV-1 backbone plasmid into 6×10^5 293T cells per well in 6-well plate. At 48 h after transfection, supernatants were collected, and then the infectivity of serially diluted pseudoviruses in the supernatants was detected in TZM-bl cells and 50 % tissue culture infectivity dose ($TCID_{50}$) was calculated. The equivalent $TCID_{50}$ inocula of pseudoviruses was added to each well of target cells (1×10^4 cells/well in 96-well plates) in the presence of the peptide inhibitor in a total volume of 100 μl supplemented with 2.5 μg/ml of DEAE (Sigma). At 48 h after viral infection, the luciferase activity was measured using a luciferase substrate (Promega, WI) on a Modulus™II microplate multimode reader (Turner Biosystems, Promega, WI).

2.6. Cell-cell fusion inhibition assay

HEK293T cells (6×10^5 cells/well) were transfected in a 6-well plate with 0.1 μg of Env expression vector, 0.6 μg of pRev, and 1 μg of pSCTZ α, and RC4 cells (6×10^5 cells/well) were transfected with 1.6 μg of pSCTZ ω in a 6-well plate. At 36 h after transfection, the HEK293T-Env effector cells were digested with EDTA, pelleted, and resuspended in DMEM. The effector cells (1×10^4 cells/well) were added to a 96-well plate. Six hours later, the target cells (RC4) were dissociated, as described above. The target cells and NPIs at various concentrations were co-cultivated with effector cells for 24 h at 37 °C, and then the cells were lysed and mixed with the luciferase substrate (Galacto-Star™ system, Applied Biosystems, Bedford, MA). Luciferase activity was measured on a Modulus™II microplate multimode reader (Turner Biosystems, Promega, WI).

2.7. Circular dichroism (CD) spectroscopy

NPIs and C34 were mixed (10 μM each) in 50 mM sodium phosphate (pH 7.0) containing 150 mM NaCl and incubated at 37 °C for 30 min before analysis. These peptide mixtures were tested at 20 °C temperature using a 1.0-nm bandwidth, 0.1-nm resolution, 0.1-cm path length, 4.0-second response time, and a 5-nm/min scanning speed using Chirascan spectropolarimeter (Applied Photophysics, UK). The spectra were corrected by subtraction of a blank corresponding to the solvent. The α-helical content was calculated from the CD signal by dividing the mean residue ellipticity at 222 nm by the value expected for 100 % helix formation (Shu et al., 2000, Yang et al., 2003). Thermal denaturation was monitored at 222 nm by applying a thermal gradient of 2 °C/min in the range of 4 °C-95 °C. Reverse melt from 95 °C to 4 °C was also detected. The melting curve was smoothed, and the midpoint of the thermal unfolding transition (Tm) value was determined using Chirascan software. The averages Tm of at least two measurements for each complex was calculated. The fraction of unfolded molecules was analyzed according to a two-state N%U mechanism.

2.8. Native page

The 6HB formed by NPI and C34 was detected by Native PAGE (He et al., 2008). The three newly designed NPIs were respectively incubated with C34 at a final concentration of 40 μM at 37 °C for 30 min. The mixture was loaded on and run in a precast 18 % Tris-glycine gel. The gel was then stained with Coomassie Blue and imaged using the GIS-2010 system (Tanon, China).

2.9. Statistical analysis

At least three independent dose-response curves were generated for each inhibitor. The IC_{50} values relative to pseudovirus alone control were calculated by nonlinear regression analysis using GraphPad Prism Software (La Jolla, CA). The mean IC_{50} was determined for each pseudovirus and inhibitor. The IC_{50} for NPIs was compared with that for N36 using a student's *t*-test with non-parametric assumption, and P values < 0.05 were considered significant.

3. Results

3.1. Peptide design and conformation simulation of NPIs

FPPR, MTQ and MTQ-FPPR were introduced into the N terminal of N36, termed FPPR-N36, MTQ-N36 and MTQ-FPPR-N36, respectively (Table 1 and Fig. 1). The molecular conformation of the NPIs was predicted using the SWISS Model and showed that three newly designed NPIs could form α-helical structures (Figure S1). All three newly designed NPIs showed no significant effect on the viability of TZM-bl cells (with the cell viability of >90 %) in the cytotoxicity analysis by CCK-8 assay using peptide concentrations ranging from 0.15625 μM to 80 μM (data not shown).

3.2. Effects of NPIs on pseudovirus infection of the different HIV-1 subtypes

The different pseudoviruses expressing Envs of HIV-1 subtype AE (SH88.6 and BJX-4.6), subtype BC (09277-R9 and BJ-28–13), subtype B (06057-C3, 06044–7 and LAI) that were spreading in China and other regions of the world were constructed to test the inhibitory activities of these NPIs. The three newly designed NPIs showed more potent inhibitory effects than N36, and their IC_{50} were 5–50-folds less than that of N36 ($P < 0.05$) (Figs. 2, 3, and Table 2).

IZ and MTQ are trimerization motifs and can promote the formation of trimers (Figure S1). MTQ-N36 showed slightly better inhibitory effects on pseudovirus than IZN36 ($P = 0.074$), but MTQ-FPPR-N36 exhibited weaker inhibitory effects than IZN36 and MTQ-N36. Compared with trimeric NPIs, monomer peptide inhibitor, FPPR-N36, showed a slightly weaker inhibitory effect. However, FPPR-N36 was effective against subtype AE pseudoviruses (BJX-4.6 and SH188.6), with similar activity with MTQ-FPPR-N36 (Fig. 2G, H, Fig. 3G, H, and Table 2). Meanwhile, the inhibitory effect of NPIs on the HIV-1 resistant strains which were selected under N36 or IZN36 co-culture, JRcsf E560K/Q577R/641I and JRcsf Q577R/648 K, were also detected.

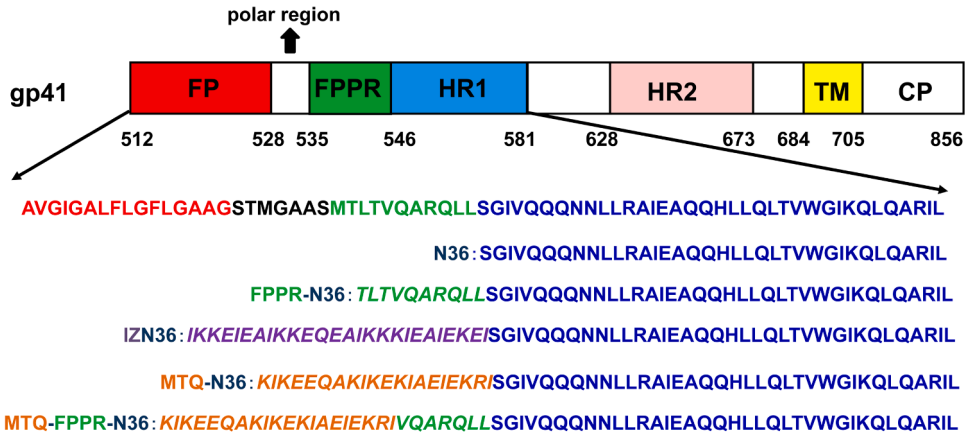

Fig. 1. Diagram of the gp41 domain. Linear representation of domains from N-terminal to C-terminal in gp41: fusion peptide (FP); fusion peptide proximal region (FPPR); N-terminal heptad repeat region (HR1); C-terminal heptad repeat region (HR2); transmembrane domain (TM); cytoplasmic tail (CP).

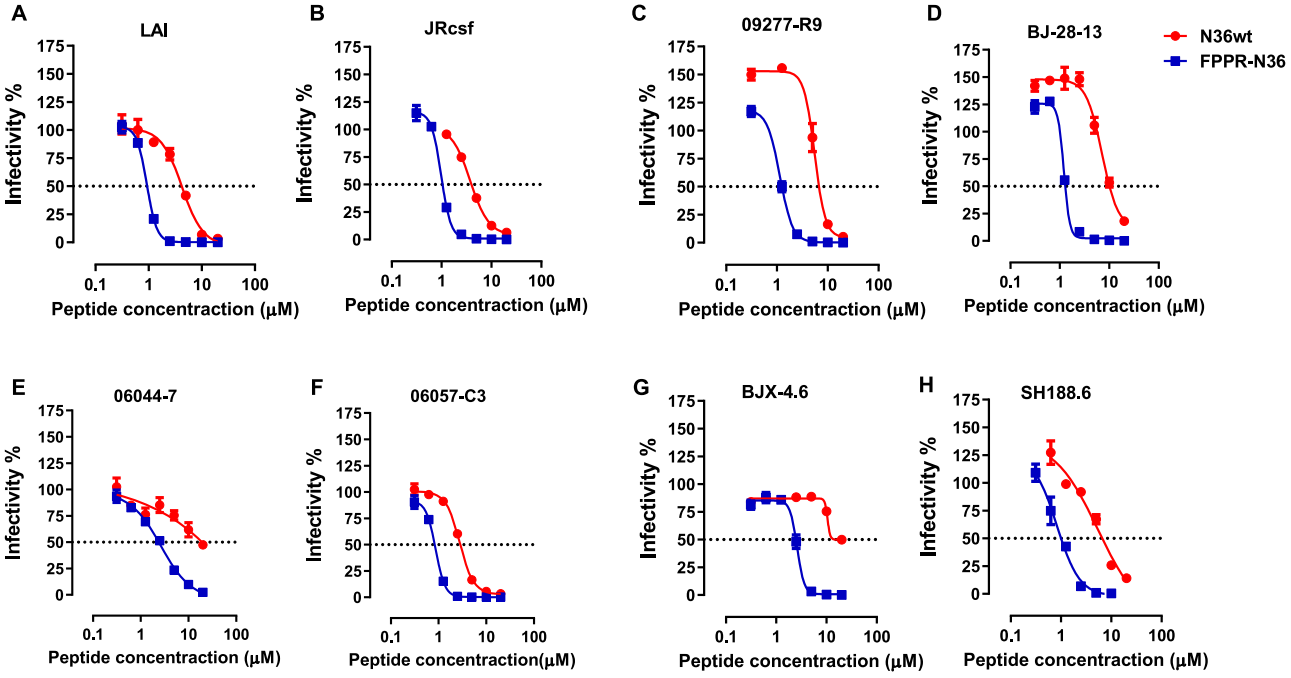

Fig. 2. The inhibitory effects of NPI monomer on pseudoviruses of different HIV-1 subtypes. The inhibitory effects of N36 and FPPR-N36 on LAI (A), JRcsf (B), 09,277-R9 (C), BJ-28–13 (D), 06,044–7 (E), 06,057-C3 (F), BJX-4.6 (G) and SH188.6 (H) were shown. The results were shown as a representative of at least three repeated experiments. Each point represents the mean of concentration ± standard deviation (SD).

Among all NPIs tested here, only FPPR-N36 showed more potency than N36 for JRcsf wild-type and two resistant viruses JRcsf E560K/Q577R/641I and JRcsf Q577R/648 K (Fig. 4 and Table 3). No inhibitory effect of MTQ-N36 or MTQ-FPPR-N36 on the two resistant viruses was observed at a peptide concentration of 1μM which was 10 times the IC_{50} in wild-type HIV (data not shown).

3.3. Inhibitory effects of NPIs on cell-cell fusion

The inhibitory effects of the three newly designed NPIs on fusion between the HIV-1 envelope-expressing cells and target cells were better than that of N36. MTQ-N36 and IZN36 had similar inhibitory effects, and MTQ-FPPR-N36 had slightly weaker inhibitory effects on cell-cell fusion. These results showed a similar trend with the pseudovirus infection assays (Table 4).

3.4. Stabilities of the coiled-coil core formed by NPIs and the 6HB formed by NPIs and C34

The introduction of FPPR, MTQ, and MTQ-FPPR may affect the formation of α-helix and the stability of the NPI itself and the 6HBs. We detected the α-helix structures of the NPIs using circular dichroism (CD) analyses. The results showed that all three newly designed NPIs could form better α-helix structures than N36, especially MTQ-N36 and MTQ-FPPR-N36 (Fig. 5A), and could also form a great α-helix of 6HB with C34. FPPR-N36 and N36 showed similar α-helicity of 6HB, but both were less than newly designed trimeric NPIs. The MTQ-N36 and MTQ-FPPR-N36 showed better α-helicity of 6HB than IZN36 (Fig. 5B). Compared with N36, the coiled-coil cores formed by newly designed NPIs displayed relatively high thermal unfolding transition (Tm) based on their thermal denaturation curves (ranging from 55 °C to 77 °C) and a △Tm was 30 °C to 50 °C, higher than that of the coiled-coil cores formed with the N36 inhibitor (Fig. 5C and Table 5). Also, the Tm value of 6HB formed by

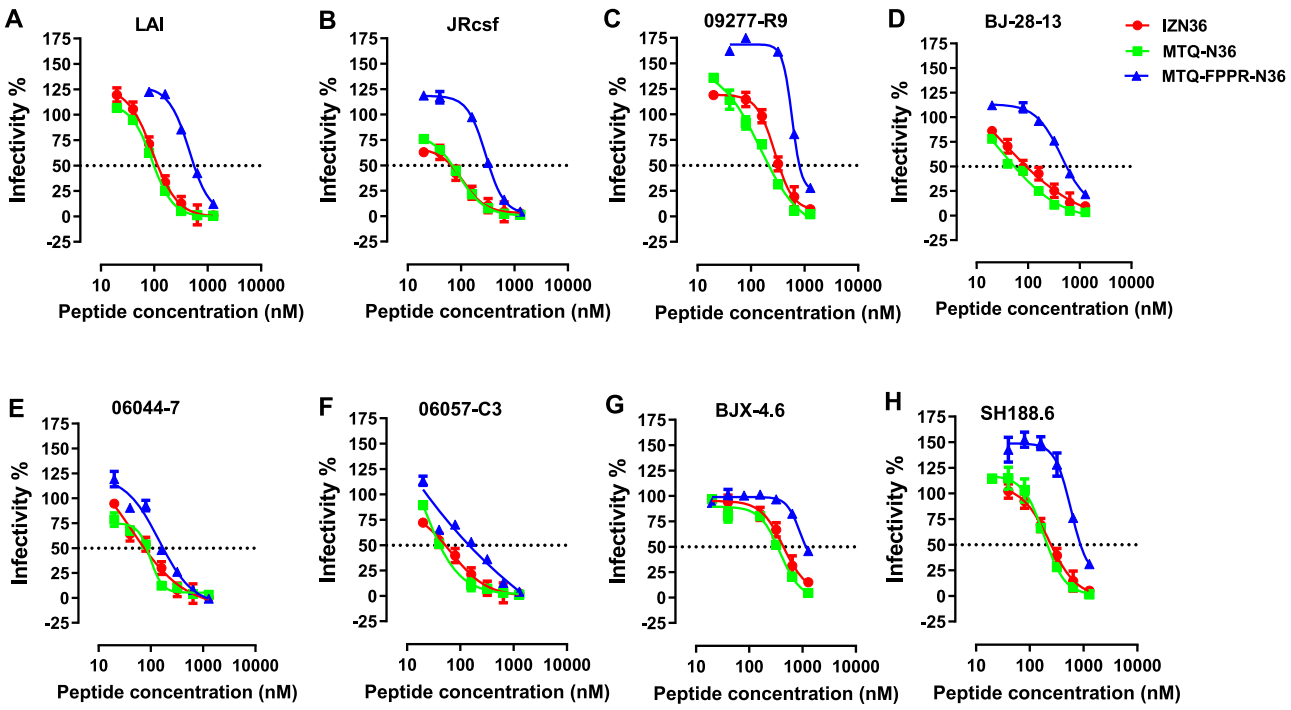

Fig. 3. The inhibitory effects of NPI trimer on pseudoviruses of different HIV −1 subtypes. The inhibitory effects of IZN36, MTQ-N36 and MTQ-FPPR-N36 on LAI (A), JRcsf (B), 09,277-R9 (C), BJ-28–13 (D), 06,044–7 (E), 06,057-C3 (F), BJX-4.6 (G) and SH188.6 (H) were shown. The results were shown as a representative of at least three repeated experiments. Each point represents the mean of concentration ± standard deviation (SD).

Table 2
The inhibitory effects of NPIs on HIV-1 Env-pseudovirus infection.

Env-pseudovirus	Subtype	N36		FPPR-N36		IZN36		MTQ-N36		MTQ-FPPR-N36	
		IC_{50} ± SD (μM)	Ratio	IC_{50} ± SD (μM)	Ratio	IC_{50} ± SD (nM)	Ratio	IC_{50} ± SD (nM)	Ratio	IC_{50} ± SD (nM)	Ratio
LAI	B	4.27±0.05	1	1.04±0.17	0.244	93.60±1.00	0.022	81.78±0.88	0.019	363.54±3.90	0.085
JRcsf	B	3.45±0.44	1	0.92±0.08	0.267	116.15±12.09	0.034	100.11±15.27	0.029	382.46±39.82	0.111
09277-R9	07BC	7.76±2.67	1	1.51±0.52	0.195	276.88±18.11	0.036	204.35±14.36	0.026	702.84±45.97	0.091
BJ-28–13	BC	8.94±2.51	1	1.25±0.06	0.139	80.38±17.87	0.009	69.66±15.49	0.008	300.90±66.90	0.034
06044–7	B	16.17±2.99	1	3.31±0.63	0.204	91.62±10.37	0.006	61.39±6.95	0.004	157.37±17.82	0.010
06057-C3	B	2.85±0.22	1	0.85±0.10	0.300	43.62±7.48	0.015	40.48±6.52	0.014	179.30±23.33	0.063
BJX-4.6	AE	19.28±0.32	1	3.15±0.73	0.160	541.80±17.73	0.028	386.9 ± 12.66	0.020	2129±69.68	0.110
SH188.6	AE	6.50±0.82	1	1.07±0.08	0.165	576.43±59.62	0.089	298.03±64.06	0.049	1337.03±298.17	0.206

The data were shown as IC_{50} ± SD. IC_{50} value was analyzed and calculated by GraphPad Prism software, and the ratio was the IC_{50} value of the newly designed NPI/the IC_{50} value of N36.

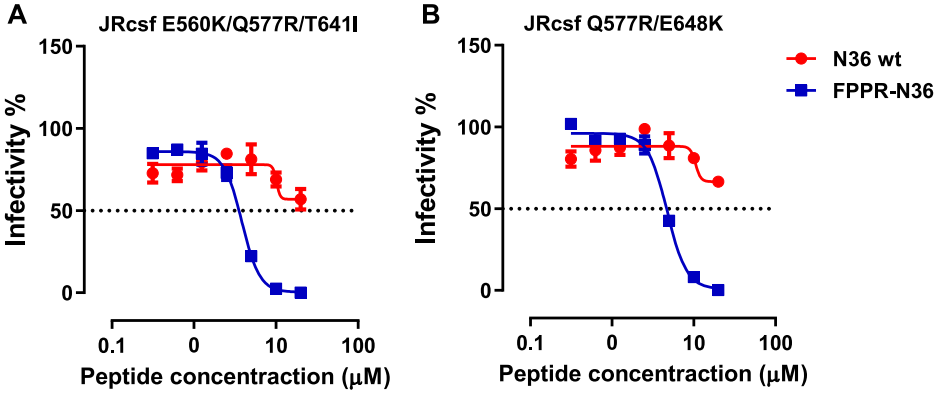

Fig. 4. The inhibitory effects of the designed NPIs on HIV-1 pseudoviruses which were resistant to N36 and IZN36. The inhibitory effects of N36 and FPPR-N36 on JRcsf E560K/Q577R/T641I (A) and JRcsf Q577R/E648 K (B) were shown. The results were shown as a representative of at least three repeated experiments. Each point represents the mean of concentration ± standard deviation (SD).

Table 3
The inhibitory effects of NPIs on HIV-1 JRcsf Env-pseudoviruses which are resistant to N36 and IZN36.

Env-pseudovirus	N36 IC_{50}± SD (μM)	Ratio	FPPR-N36 IC_{50} ± SD (μM)	Ratio
JRcsf	3.45±0.44	1	0.92±0.08	1
JRcsf E560K/Q577R/T641I	>20	>5.797	3.65±0.26	3.967
JRcsf Q577R/E648K	>20	>5.797	4.08±0.91	4.434

The data were shown as IC_{50} ± SD. The IC_{50} value was analyzed and calculated by GraphPad Prism software, and the ratio was the IC_{50} value of the newly designed NPI/the IC_{50} value of N36.

newly designed NPIs and C34 was better than that by N36/C34 or IZN36/C34 (ranging from 76.5 °C to 83 °C) and the △Tm was 24.5 °C to 31 °C, higher than that of the 6HB formed with the N36 inhibitor, especially that containing MTQ-N36 and MTQ-FPPR-N36 (Fig. 5D and Table 5).

3.5. Effects of NPIs and C34 interactions by native page

The 6HBs formed by all five NPIs and C34 were visualized by Native PAGE and the results were consistent with CD analyses. IZN36/C34 formed more polymers, while MTQ-N36/C34 and MTQ-FPPR-N36/C34 did not, and both of them showed a higher proportion of 6HB than FPPR-N36/C34 and IZN—N36/C34, indicating that the coiled-coil cores or 6HBs formed by two newly designed MTQ-engineered trimeric

Table 5
The thermal denaturation of coiled-coil cores formed by the NPIs and the six-helix bundles (6HB) formed by mixtures of the NPIs and C34.

NPIs	Six-helix bundle (NPI-C34)		Coiled-coil core (NPI)	
	Tm (°C)	△Tm (°C)	Tm (°C)	△Tm (°C)
N36wt	52		25	
FPPR-N36	76.5	24.5	55	30
IZN36	73	21	65	40
MTQ-N36	80	28	75	50
MTQ-FPPR-N36	83	31	77	52

Table 4
The inhibitory effects of NPIs on cell-cell fusion.

Env	N36		FPPR-N36		IZN36		MTQ-N36		MTQ-FPPR-N36	
	IC_{50} ± SD (μM)	Ratio	IC_{50} ± SD (μM)	Ratio	IC_{50} ± SD (nM)	Ratio	IC_{50} ± SD (nM)	Ratio	IC_{50} ± SD (nM)	Ratio
LAI	3.58±0.30	1	1.41±0.12	0.394	95.61±6.99	0.027	116.54±8.52	0.033	298±21.78	0.083
09277-R9	2.68±1.52	1	0.42±0.24	0.157	31.43±10.20	0.012	22.44±2.66	0.008	64.25±7.61	0.024
06044–7	2.10±0.32	1	0.50±0.08	0.238	45.76±30.19	0.022	40.09±26.45	0.019	116.67±76.96	0.056
06057-C3	5.61±1.00	1	0.84±0.11	0.150	182.40±1.84	0.033	102.11±24.6	0.018	251.95±16.05	0.045

The data were shown as IC_{50} ± SD. The IC_{50} value was analyzed and calculated by GraphPad Prism software, and the ratio was the IC_{50} value of the newly designed NPI/the IC_{50} value of N36.

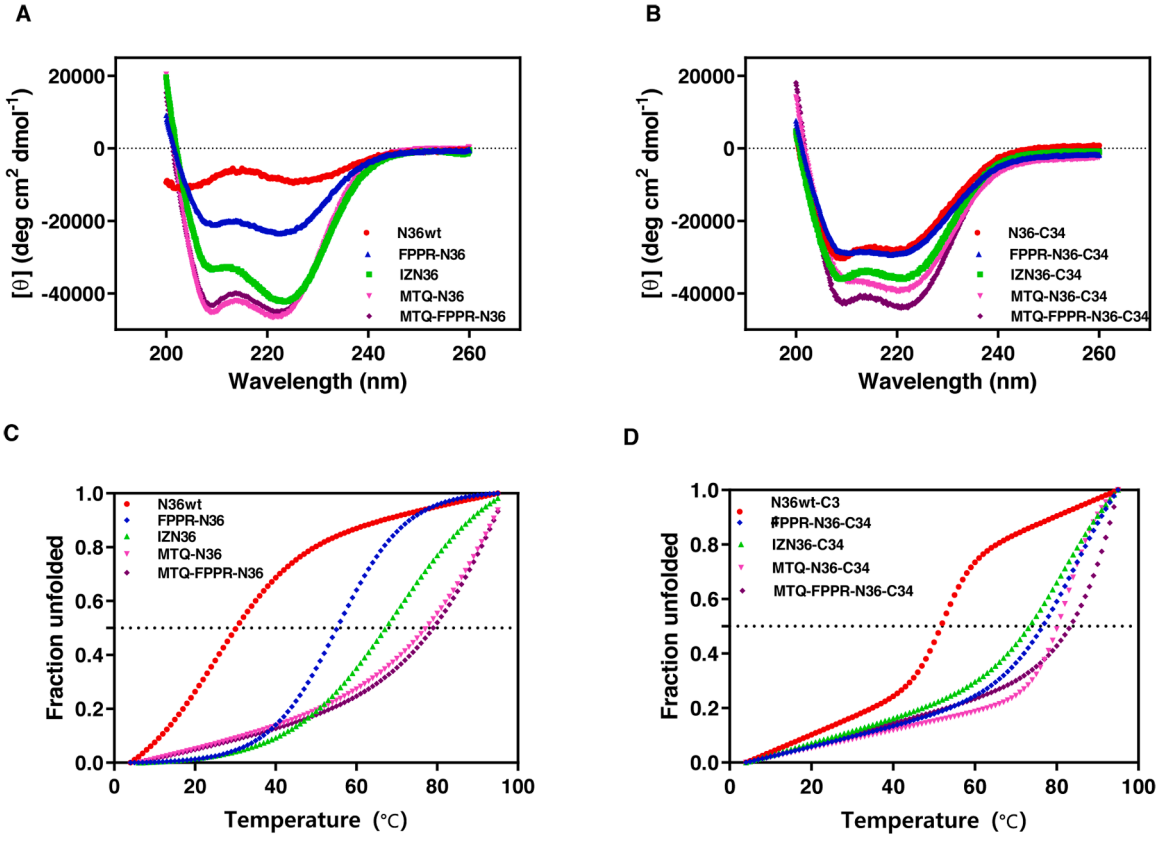

Fig. 5. The α-helicity and thermal denaturation of the coiled-coil cores formed by NPIs and the six-helix bundles (6HBs) formed by NPIs and C34. The α-helicities of the coiled-coil cores (A) and the 6HBs (B) and the thermostabilities of the coiled-coil cores (C) and the 6HBs (D) were determined using CD spectroscopy.

inhibitors were more stable (Fig. 6).

4. Discussions

The heptad-repeat regions of HIV-1 gp41 provide a target for the development of new anti-HIV-1 inhibitors. Fusion peptide inhibitors are divided into N and C peptide inhibitors (NPIs & CPIs) due to the different origin sites.

The CPIs bind to HR1 to prevent the formation of endogenous 6HB. In clinical application, viral HR1, especially GIV motif ($gp_{547–549}$), tends to mutation, and HR2 is accompanied by mutations to adapt to HR1. However, the sequence of the CPI does not change, causing its significantly reduced binding affinity to virus HR. Mutations in HR1 may also increase steric hindrance or generate electrostatic repulsion, leading to a decrease in the inhibitory effect of CPIs (Loutfy et al., 2007).

NPI monomers have two targets of gp41, Firstly, it can bind to HR2, thereby inhibiting the formation of endogenous 6HB. Secondly, they can interact with the HR1 of gp41 through monomer or dimer interactions, leading to the formation of a heterotrimeric coiled-coil core that interferes with the assembly of endogenous gp41 coiled-coil core. The advantage of N-peptide lies in its ability to target two distinct sites associated with HIV fusion and entry (Zhuang et al., 2019, Zhuang et al., 2012, Shu et al., 2000, He et al., 2008). However, due to their poor solubility and low bioavailability, NPIs tend to aggregate and exhibit limited IC_{50} values at the micromolar level. Notably, it has been reported that IZN36 formed by combining monomeric N36 with the trimer motif IZ, significantly enhances solubility and inhibitory potency at the nanomolar level (Eckert and Kim, 2001). In addition, NPIs covNHR3 and N35CCG-N13 were developed, and the IC_{50} was also at nanomolar level (Louis et al., 2003, Crespillo et al., 2014). In the previous study, we also found that NPIs-resistant viruses selected two genetic pathways that contain an early mutation in HR1 or HR2 with equal probability to escape from N36 and preferentially selected the HR1 pathway to escape from IZN36 (Zhuang et al., 2019, Zhuang et al., 2012), the reasons may involve the two binding sites for NPI monomer and one binding site for NPI trimer. The N36-resistant viruses are difficult to culture to increase the resistant degree, implying that HIV-1 may not easily replicate in the presence of the NPI monomer. Therefore, current research on NPIs primarily focuses on optimizing their inhibitory effects against HIV-1.

In this study, the design strategies of new NPIs include increasing the solubility of monomer and the stability of the trimer to enhance the inhibitory potential. The main way of increasing solubility is to add polar hydrophilic amino acids. Fusion peptide (FP) is located at the N terminus of gp41. It contains hydrophobic amino acids which can be inserted into the cell membrane (Fig. 1). FP23 is the most widely used FP model ($gp41_{512–534}$) was designed by adding 7 additional polar amino acids to FP16 ($gp41_{512–527}$) (Charloteaux et al., 2006, Lai and Freed, 2014). FP33 is composed of FP23 and FPPR. The ability of FPPR ($gp41_{536–545}$) to increase solubility of peptides has been reported (Cai et al., 2011). Therefore, we introduced the partial FPPR sequence to form 2.5 turns of α-helix, aiming to increase the hydrophilicity of the inhibitor.

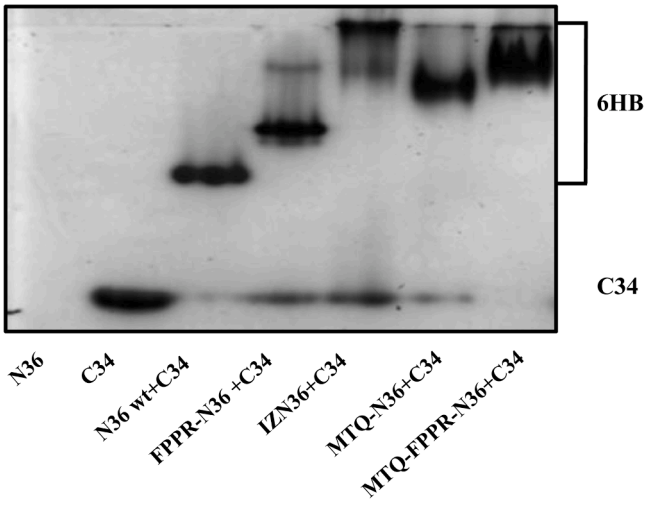

Fig. 6. The 6HBs formed by the NPIs and C34 were shown in Native-PAGE. Final concentrations of N and C peptides were 40 μM. The gel was stained by Coomassie Blue.

Introducing the trimer motif increases the stability of the trimer, thereby increasing the inhibitory potential of the NPI. The HR1 is an α-helix structure with 3.6 amino acid residues in one helix, and every 7 amino acids has one leucine, so these leucines will appear on the same side, parallel to the spiral axis. This is also the main reason why monomeric NPIs tend to aggregate to form polymers in solution. IZ contains a heptad repeat region, similar to Ile-Glu-Lys-Lys-Ile-Glu-Ala (d-e-f-g-a-b-c) (Eckert and Kim, 2001). These charged amino acid residues form electrostatic interaction with the amino acid residues of the adjacent helix, and the glutamic acid at position b forms a salt bridge with the lysine at position f in the same helix, which improves the stability of the trimeric coiled-coil core. MTQ is designed by our group and makes α-helix to form a stable trimeric coiled-coil structure because of containing several Glu and Lys (Wang et al., 2011). Therefore, we constructed NPI MTQ-N36 and MTQ-FPPR-N36, composed of MTQ, FPPR, and N36, respectively. Structure prediction showed that these NPIs can form a complete α-helix.

The properties and inhibitory effects of the three designed NPIs were verified through different inhibitory experiments. According to the results of inhibitory assays, we found that the three newly designed NPIs showed more potent inhibitory effects than N36, and FPPR-N36 showed better inhibitory effects on N36- and IZN36-resistance strains, which provides the possibility for the subsequent optimization, application, and development (Fig. 4 and Table 3).

The mechanisms of different inhibitory effects of NPIs were analyzed using CD and native PAGE. The results showed that the α-helicity of all three new NPIs in the coiled-coil core or the 6HB is better than the corresponding monomeric N36 or trimeric IZN36 (Fig. 5A, B). Compared with N36, the designed NPIs form more stable coiled-coil cores with Tm values ranging from 55 °C to 77 °C, and the 6HB formed by C34 and new NPIs displayed relatively high transition midpoints (Tm) (ranging from 76.5 °C to 83 °C), indicating that the new NPIs had better thermostability than the corresponding monomeric N36 or trimeric IZN36 (Fig. 5C, D and Table 5).

FPPR-N36 showed a better inhibitory effect than N36, the reason may be the increased peptide solubility due to the addition of hydrophilic residues (Cai et al., 2011), and the better stability of the coiled-coil core and 6HB. FPPR-N36 was the only tested NPIs that inhibited the N36- and IZN36-resistant strains, reminding us that an appropriate increase in the length of peptide binding sites may prevent viral escape. The inhibitory effect of MTQ-N36 on different strains was better than that of IZN36, the mechanisms may include the α-helicity formation and stability of MTQ-N36 coiled-coil core itself and the 6HB were better than that of IZN36. NPIs have a short contact time with HR2 due to the instantaneous exposure of HR2, while MTQ-FPPR-N36 has a longer sequence and larger steric hindrance, which may interfere with its binding to HR2, therefore, MTQ-FPPR-N36 is less effective than MTQ-N36 and IZN36.

4. Conclusions

In our study, N36 was modified by introducing FPPR and/or the trimer motif MTQ. Three newly designed NPIs showed better inhibitory effects and the IC_{50} of trimeric NPIs reached the nanomolar level. The FPPR-N36 can also inhibit the NPIs-resistant HIV-1 strains. Meanwhile, NPIs are characterized by genetic conservation and drug sensitivity, therefore they have good clinical application prospects. This study

provided new insight for the development of more broad-spectrum effective peptide inhibitors.

5. Patents

The patent granted in China No ZL 2021 1 0246647.2 resulted from the work reported in this manuscript.

Informed consent statement

Not applicable.

CRediT authorship contribution statement

Chen Yuan: Methodology, Investigation, Data curation, Writing – original draft. **Jia-Ye Wang:** Methodology, Investigation, Writing – original draft. **Bu-Yi Wang:** Methodology. **Yi-Lin Zhao:** Methodology. **Yan Li:** Methodology. **Di Li:** Investigation. **Hong Ling:** Writing – review & editing. **Min Zhuang:** Conceptualization, Visualization, Supervision, Writing – review & editing.

Declaration of competing interest

The authors declare that they have no known competing financial interests or personal relationships that could have appeared to influence the work reported in this paper.

Acknowledgments

We thank the associated professor, Yuan Yao (School of Chemistry and Chemical Engineering, Harbin Institute of Technology, Harbin, China), for analyzing molecular structures.

Funding

This work was supported by the National Natural Science Foundation of China (81201321 and 81871654), and Key Projects in the National Science & Technology Pillar Program during the thirteenth Five-Year Plan Period (2018ZX10731101-002-004).

Supplementary materials

Supplementary material associated with this article can be found, in the online version, at doi:10.1016/j.crmicr.2025.100364.

Data availability

All data generated or analyzed during this study are included in this published article and its supplementary information files.

References

[1] Wyatt, R., Kwong, P.D., Desjardins, E., Sweet, R.W., Robinson, J., Hendrickson, W. A., Sodroski, J.G., 1998. The antigenic structure of the HIV gp120 envelope glycoprotein. Nature 393, 705–711. https://doi.org/10.1038/31514.

[2] Pancera, M., Majeed, S., Ban, Y.E., Chen, L., Huang, C.C., Kong, L., Kwon, Y.D., Stuckey, J., Zhou, T., Robinson, J.E., Schief, W.R., Sodroski, J., Wyatt, R., Kwong, P. D., 2010. Structure of HIV-1 gp120 with gp41-interactive region reveals layered envelope architecture and basis of conformational mobility. Proc. Natl. Acad. Sci. U S A 107, 1166–1171. https://doi.org/10.1073/pnas.0911004107.

[3] Huang, C.C., Tang, M., Zhang, M.Y., Majeed, S., Montabana, E., Stanfield, R.L., Dimitrov, D.S., Korber, B., Sodroski, J., Wilson, I.A., Wyatt, R., Kwong, P.D., 2005. Structure of a V3-containing HIV-1 gp120 core. Science (1979) 310, 1025–1028. https://doi.org/10.1126/science.1118398.

[4] Zhou, T., Xu, L., Dey, B., Hessell, A.J., Van Ryk, D., Xiang, S.H., Yang, X., Zhang, M. Y., Zwick, M.B., Arthos, J., Burton, D.R., Dimitrov, D.S., Sodroski, J., Wyatt, R., Nabel, G.J., Kwong, P.D., 2007. Structural definition of a conserved neutralization epitope on HIV-1 gp120. Nature 445, 732–737. https://doi.org/10.1038/nature05580.

[5] Kwong, P.D., Wyatt, R., Robinson, J., Sweet, R.W., Sodroski, J., Hendrickson, W.A., 1998. Structure of an HIV gp120 envelope glycoprotein in complex with the CD4 receptor and a neutralizing human antibody. Nature 393, 648–659. https://doi.org/10.1038/31405.

[6] Pancera, M., Zhou, T., Druz, A., Georgiev, I.S., Soto, C., Gorman, J., Huang, J., Acharya, P., Chuang, G.Y., Ofek, G., Stewart-Jones, G.B., Stuckey, J., Bailer, R.T., Joyce, M.G., Louder, M.K., Tumba, N., Yang, Y., Zhang, B., Cohen, M.S., Haynes, B. F., Mascola, J.R., Morris, L., Munro, J.B., Blanchard, S.C., Mothes, W., Connors, M., Kwong, P.D., 2014. Structure and immune recognition of trimeric pre-fusion HIV-1 Env. Nature 514, 455–461. https://doi.org/10.1038/nature13808.

[7] Buzon, V., Natrajan, G., Schibli, D., Campelo, F., Kozlov, M.M., Weissenhorn, W., 2010. Crystal structure of HIV-1 gp41 including both fusion peptide and membrane proximal external regions. PLoS. Pathog. 6, e1000880. https://doi.org/10.1371/journal.ppat.1000880.

[8] Chan, D.C., Fass, D., Berger, J.M., Kim, P.S., 1997. Core structure of gp41 from the HIV envelope glycoprotein. Cell 89, 263–273. https://doi.org/10.1016/s0092-8674(00)80205-6.

[9] Lu, M., Kim, P.S., 1997. A trimeric structural subdomain of the HIV-1 transmembrane glycoprotein. J. Biomol. Struct. Dyn. 15, 465–471. https://doi.org/10.1080/07391102.1997.10508958.

[10] Caffrey, M., 2001. Model for the structure of the HIV gp41 ectodomain: insight into the intermolecular interactions of the gp41 loop. Biochim. Biophys. Acta 1536, 116–122.

[11] Markosyan, R.M., Cohen, F.S., Melikyan, G.B., 2003. HIV-1 envelope proteins complete their folding into six-helix bundles immediately after fusion pore formation. Mol. Biol. Cell 14, 926–938.

[12] Eckert, D.M., Kim, P.S., 2001a. Mechanisms of viral membrane fusion and its inhibition. Annu. Rev. Biochem. 70, 777–810. https://doi.org/10.1146/annurev.biochem.70.1.777.

[13] Nelson, J.D., Brunel, F.M., Jensen, R., Crooks, E.T., Cardoso, R.M., Wang, M., Hessell, A., Wilson, I.A., Binley, J.M., Dawson, P.E., Burton, D.R., Zwick, M.B., 2007. An affinity-enhanced neutralizing antibody against the membrane-proximal external region of human immunodeficiency virus type 1 gp41 recognizes an epitope between those of 2F5 and 4E10. J. Virol. 81, 4033–4043. https://doi.org/10.1128/JVI.02588-06.

[14] Caffrey, M., 2011. HIV envelope: challenges and opportunities for development of entry inhibitors. Trends. Microbiol. 19, 191–197. https://doi.org/10.1016/j.tim.2011.02.001.

[15] Wild, C., Greenwell, T., Matthews, T., 1993. A synthetic peptide from HIV-1 gp41 is a potent inhibitor of virus-mediated cell-cell fusion. AIDS Res. Hum. Retroviruses 9, 1051–1053. https://doi.org/10.1089/aid.1993.9.1051.

[16] Jiang, S., Lin, K., Strick, N., Neurath, A.R., 1993. Inhibition of HIV-1 infection by a fusion domain binding peptide from the HIV-1 envelope glycoprotein GP41. Biochem. Biophys. Res. Commun. 195, 533–538. https://doi.org/10.1006/bbrc.1993.2078.

[17] Moore, J.P., Doms, R.W., 2003. The entry of entry inhibitors: a fusion of science and medicine. Proc. Natl. Acad. Sci. U S. A 100, 10598–10602. https://doi.org/10.1073/pnas.1932511100.

[18] He, Y., 2013. Synthesized peptide inhibitors of HIV-1 gp41-dependent membrane fusion. Curr. Pharm. Des. 19, 1800–1809. https://doi.org/10.2174/1381612811319100004.

[19] Baldwin, C.E., Sanders, R.W., Deng, Y., Jurriaans, S., Lange, J.M., Lu, M., Berkhout, B., 2004. Emergence of a drug-dependent human immunodeficiency virus type 1 variant during therapy with the T20 fusion inhibitor. J. Virol. 78, 12428–12437. https://doi.org/10.1128/JVI.78.22.12428-12437.2004.

[20] Joly, V., Jidar, K., Tatay, M., Yeni, P., 2010. Enfuvirtide: from basic investigations to current clinical use. Expert. Opin. PharmacOther 11, 2701–2713. https://doi.org/10.1517/14656566.2010.522178.

[21] McGillick, B.E., Balius, T.E., Mukherjee, S., Rizzo, R.C., 2010. Origins of resistance to the HIVgp41 viral entry inhibitor T20. Biochemistry 49, 3575–3592. https://doi.org/10.1021/bi901915g.

[22].<2004-AIDS Rev-discontinuation of the clinical development of fusion inhibitor T1249.pdf>.

[23] Dwyer, J.J., Wilson, K.L., Davison, D.K., Freel, S.A., Seedorff, J.E., Wring, S.A., Tvermoes, N.A., Matthews, T.J., Greenberg, M.L., Delmedico, M.K., 2007. Design of helical, oligomeric HIV-1 fusion inhibitor peptides with potent activity against enfuvirtide-resistant virus. Proc. Natl. Acad. Sci. 104, 12772–12777. https://doi.org/10.1073/pnas.0701478104.

[24] Nishikawa, H., Oishi, S., Fujita, M., Watanabe, K., Tokiwa, R., Ohno, H., Kodama, E., Izumi, K., Kajiwara, K., Naitoh, T., Matsuoka, M., Otaka, A., Fujii, N., 2008. Identification of minimal sequence for HIV-1 fusion inhibitors. Bioorg. Med. Chem. 16, 9184–9187. https://doi.org/10.1016/j.bmc.2008.09.018.

[25] Chong, H., Yao, X., Qiu, Z., Qin, B., Han, R., Waltersperger, S., Wang, M., Cui, S., He, Y., 2012a. Discovery of critical residues for viral entry and inhibition through structural insight of HIV-1 fusion inhibitor CP621–652. J. Biol. Chem. 287, 20281–20289. https://doi.org/10.1074/jbc.M112.354126.

[26] Chong, H., Yao, X., Sun, J., Qiu, Z., Zhang, M., Waltersperger, S., Wang, M., Cui, S., He, Y., 2012b. The M-T hook structure is critical for design of HIV-1 fusion inhibitors. J. Biol. Chem. 287, 34558–34568. https://doi.org/10.1074/jbc.M112.390393.

[27] Chong, H., Qiu, Z., Sun, J., Qiao, Y., Li, X., He, Y., 2014. Two M-T hook residues greatly improve the antiviral activity and resistance profile of the HIV-1 fusion inhibitor SC29EK. Retrovirology. 11. https://doi.org/10.1186/1742-4690-11-40.

[28] Zheng, B., Wang, K., Lu, L., Yu, F., Cheng, M., Jiang, S., Liu, K., Cai, L., 2014. Hydrophobic mutations in buried polar residues enhance HIV-1 gp41 N-terminal

heptad repeat–C-terminal heptad repeat interactions and C-peptides' anti-HIV activity. AIDS 28, 1251–1260. https://doi.org/10.1097/qad.0000000000000255.
[29] Chong, H., Qiu, Z., Su, Y., He, Y., 2015a. The N-terminal T–T motif of a third-generation HIV-1 fusion inhibitor is not required for binding affinity and antiviral activity. J. Med. Chem. 58, 6378–6388. https://doi.org/10.1021/acs.jmedchem.5b00109.
[30] Chong, H., Qiu, Z., Su, Y., Yang, L., He, Y., 2015b. Design of a highly potent HIV-1 fusion inhibitor targeting the gp41 pocket. AIDS 29, 13–21. https://doi.org/10.1097/qad.0000000000000498.
[31] Chong, H., Wu, X., Su, Y., He, Y., 2016. Development of potent and long-acting HIV-1 fusion inhibitors. AIDS 30, 1187–1196. https://doi.org/10.1097/qad.0000000000001073.
[32] Chong, H., Xue, J., Xiong, S., Cong, Z., Ding, X., Zhu, Y., Liu, Z., Chen, T., Feng, Y., He, L., Guo, Y., Wei, Q., Zhou, Y., Qin, C., He, Y., Kirchhoff, F., 2017. A lipopeptide HIV-1/2 fusion inhibitor with highly PotentIn vitro,ex vivo, andIn VivoAntiviral activity. J. Virol. 91. https://doi.org/10.1128/jvi.00288-17.
[33] Ding, X., Zhang, X., Chong, H., Zhu, Y., Wei, H., Wu, X., He, J., Wang, X., He, Y., Kirchhoff, F., 2017. Enfuvirtide (T20)-based lipopeptide is a potent HIV-1 cell fusion inhibitor: implications for viral entry and inhibition. J. Virol. 91. https://doi.org/10.1128/jvi.00831-17.
[34] Xue, J., Chong, H., Zhu, Y., Zhang, J., Tong, L., Lu, J., Chen, T., Cong, Z., Wei, Q., He, Y., 2022. Efficient treatment and pre-exposure prophylaxis in rhesus macaques by an HIV fusion-inhibitory lipopeptide. Cell 185, 131–144. https://doi.org/10.1016/j.cell.2021.11.032 e18.
[35] Chong, H., Yao, X., Zhang, C., Cai, L., Cui, S., Wang, Y., He, Y., 2012c. Biophysical property and broad anti-HIV activity of albuvirtide, a 3-maleimimidopropionic acid-modified peptide fusion inhibitor. PLoS. One 7, e32599. https://doi.org/10.1371/journal.pone.0032599.
[36] Greenberg, M.L., Cammack, N., 2004. Resistance to enfuvirtide, the first HIV fusion inhibitor. J. Antimicrob. Chemother 54, 333–340. https://doi.org/10.1093/jac/dkh330.
[37] Wild, C.T., Shugars, D.C., Greenwell, T.K., McDanal, C.B., Matthews, T.J., 1994. Peptides corresponding to a predictive alpha-helical domain of human immunodeficiency virus type 1 gp41 are potent inhibitors of virus infection. Proc. Natl. Acad. Sci. 91, 9770–9774. https://doi.org/10.1073/pnas.91.21.9770.
[38] De Feo, C.J., Weiss, C.D., 2012. Escape from human immunodeficiency virus type 1 (HIV-1) entry inhibitors. Viruses. 4, 3859–3911.
[39] Liu, Z., Shan, M., Li, L., Lu, L., Meng, S., Chen, C., He, Y., Jiang, S., Zhang, L., 2011. In vitro selection and characterization of HIV-1 variants with increased resistance to sifuvirtide, a novel HIV-1 fusion inhibitor. J. Biol. Chem. 286, 3277–3287. https://doi.org/10.1074/jbc.M110.199323.
[40] Lu, J., Deeks, S.G., Hoh, R., Beatty, G., Kuritzkes, B.A., Martin, J.N., Kuritzkes, D. R., 2006. Rapid emergence of enfuvirtide resistance in HIV-1-infected patients: results of a clonal analysis. J. Acquir. Immune Defic. Syndr. 43, 60–64. https://doi.org/10.1097/01.qai.0000234083.34161.55.
[41] Eckert, D.M., Kim, P.S., 2001b. Design of potent inhibitors of HIV-1 entry from the gp41 N-peptide region. Proc. Natl. Acad. Sci. U S A 98, 11187–11192. https://doi.org/10.1073/pnas.201392898.
[42] Izumi, K., Nakamura, S., Nakano, H., Shimura, K., Sakagami, Y., Oishi, S., Uchiyama, S., Ohkubo, T., Kobayashi, Y., Fujii, N., Matsuoka, M., Kodama, E.N., 2010. Characterization of HIV-1 resistance to a fusion inhibitor, N36, derived from the gp41 amino-terminal heptad repeat. Antiviral Res. 87, 179–186. https://doi.org/10.1016/j.antiviral.2010.04.011.
[43] Zhuang, M., Vassell, R., Yuan, C., Keller, P.W., Ling, H., Wang, W., Weiss, C.D., 2019. Mutations that increase the stability of the postfusion gp41 conformation of the HIV-1 envelope glycoprotein are selected by both an X4 and R5 HIV-1 virus to escape fusion inhibitors corresponding to heptad repeat 1 of gp41, but the gp120 adaptive Mutations differ between the two viruses. J. Virol. 93. https://doi.org/10.1128/JVI.00142-19.
[44] Zhuang, M., Wang, W., De Feo, C.J., Vassell, R., Weiss, C.D., 2012. Trimeric, coiled-coil extension on peptide fusion inhibitor of HIV-1 influences selection of resistance pathways. J. Biol. Chem. 287, 8297–8309. https://doi.org/10.1074/jbc.M111.324483.
[45] Shu, W., Liu, J., Ji, H., Radigen, L., Jiang, S., Lu, M., 2000. Helical interactions in the HIV-1 gp41 core reveal structural basis for the inhibitory activity of gp41 peptides. Biochemistry 39, 1634–1642.
[46] He, Y., Cheng, J., Li, J., Qi, Z., Lu, H., Dong, M., Jiang, S., Dai, Q., 2008. Identification of a critical motif for the human immunodeficiency virus type 1 (HIV-1) gp41 core structure: implications for designing novel anti-HIV fusion inhibitors. J. Virol. 82, 6349–6358. https://doi.org/10.1128/JVI.00319-08.
[47] Bewley, C.A., Louis, J.M., Ghirlando, R., Clore, G.M., 2002a. Design of a novel peptide inhibitor of HIV fusion that disrupts the internal trimeric coiled-coil of gp41. J. Biol. Chem. 277, 14238–14245. https://doi.org/10.1074/jbc.M201453200.
[48] Bewley, C.A., Louis, J.M., Ghirlando, R., Clore, G.M., 2002b. Design of a novel peptide inhibitor of HIV fusion that disrupts the internal trimeric coiled-coil of gp41. J. Biol. Chem. 277, 14238–14245. https://doi.org/10.1074/jbc.M201453200.
[49] Louis, J.M., Nesheiwat, I., Chang, L., Clore, G.M., Bewley, C.A., 2003. Covalent trimers of the internal N-terminal trimeric coiled-coil of gp41 and antibodies directed against them are potent inhibitors of HIV envelope-mediated cell fusion. J. Biol. Chem. 278, 20278–20285. https://doi.org/10.1074/jbc.M301627200.
[50] Crespillo, S., Cámara-Artigas, A., Casares, S., Morel, B., Cobos, E.S., Mateo, P.L., Mouz, N., Martin, C.E., Roger, M.G., El Habib, R., Su, B., Moog, C., Conejero-Lara, F., 2014a. Single-chain protein mimetics of the N-terminal heptad-repeat region of gp41 with potential as anti–HIV-1 drugs. In: Proceedings of the National Academy of Sciences, 111, pp. 18207–18212. https://doi.org/10.1073/pnas.1413592112.
[51] Yuan, C., Wang, J.Y., Zhao, H.J., Li, Y., Li, D., Ling, H., Zhuang, M., 2019. Mutations of Glu560 within HIV-1 envelope glycoprotein N-terminal heptad repeat region contribute to resistance to peptide inhibitors of virus entry. Retrovirology. 16, 36. https://doi.org/10.1186/s12977-019-0496-8.
[52] Wang, J.Y., Song, W.T., Li, Y., Chen, W.J., Yang, D., Zhong, G.C., Zhou, H.Z., Ren, C.Y., Yu, H.T., Ling, H., 2011. Improved expression of secretory and trimeric proteins in mammalian cells via the introduction of a new trimer motif and a mutant of the tPA signal sequence. Appl. Microbiol. Biotechnol. 91, 731–740. https://doi.org/10.1007/s00253-011-3297-0.
[53] Platt, E.J., Wehrly, K., Kuhmann, S.E., Chesebro, B., Kabat, D., 1998. Effects of CCR5 and CD4 cell surface concentrations on infections by macrophagetropic isolates of human immunodeficiency virus type 1. J. Virol. 72, 2855–2864. https://doi.org/10.1128/JVI.72.4.2855-2864.1998.
[54] Yang, H., Lan, C., Xiao, Y., Chen, Y.H., 2003. Antibody to CD14 like CXCR4-specific antibody 12G5 could inhibit CXCR4-dependent chemotaxis and HIV Env-mediated cell fusion. Immunol. Lett. 88, 27–30.
[55] Loutfy, M.R., Raboud, J.M., Montaner, J.S., Antoniou, T., Wynhoven, B., Smaill, F., Rouleau, D., Gill, J., Schlech, W., Brumme, Z.L., Mo, T., Gough, K., Rachlis, A., Harrigan, P.R., Walmsley, S.L., 2007. Assay of HIV gp41 amino acid sequence to identify baseline variation and mutation development in patients with virologic failure on enfuvirtide. Antiviral Res. 75, 58–63. https://doi.org/10.1016/j.antiviral.2006.11.011.
[56] Crespillo, S., Camara-Artigas, A., Casares, S., Morel, B., Cobos, E.S., Mateo, P.L., Mouz, N., Martin, C.E., Roger, M.G., El Habib, R., Su, B., Moog, C., Conejero-Lara, F., 2014b. Single-chain protein mimetics of the N-terminal heptad-repeat region of gp41 with potential as anti-HIV-1 drugs. Proc. Natl. Acad. Sci. U S A 111, 18207–18212. https://doi.org/10.1073/pnas.1413592112.
[57] Charloteaux, B., Lorin, A., Crowet, J.M., Stroobant, V., Lins, L., Thomas, A., Brasseur, R., 2006. The N-terminal 12 residue long peptide of HIV gp41 is the minimal peptide sufficient to induce significant T-cell-like membrane destabilization in vitro. J. Mol. Biol. 359, 597–609. https://doi.org/10.1016/j.jmb.2006.04.018.
[58] Lai, A.L., Freed, J.H., 2014. HIV gp41 fusion peptide increases membrane ordering in a cholesterol-dependent fashion. Biophys. J. 106, 172–181. https://doi.org/10.1016/j.bpj.2013.11.027.
[59] Cai, L., Gochin, M., Liu, K., 2011. Biochemistry and biophysics of HIV-1 gp41 - membrane interactions and implications for HIV-1 envelope protein mediated viral-cell fusion and fusion inhibitor design. Curr. Top. Med. Chem. 11, 2959–2984. https://doi.org/10.2174/156802611798808497.